

Role of the Entangled Amorphous Network in Tensile Deformation of Semicrystalline Polymers

Yongfeng Men* and Jens Rieger

BASF Aktiengesellschaft, Polymer Physics, 67056 Ludwigshafen, Germany

Gert Strobl

Physikalisches Institut der Albert-Ludwigs-Universität, 79104 Freiburg, Germany

(Received 7 March 2003; published 29 August 2003)

Being composed of crystalline lamellae and entangled amorphous polymeric chains in between, semicrystalline polymers always show a complicated deformation behavior under tensile deformation. In recent years, the process of tensile deformation was found to exhibit several regimes: intralamellar slipping of crystalline blocks occurs at small deformation whereas a stress-induced crystalline block disaggregation-recrystallization process occurs at a strain larger than the yield strain. The strain at this transition point is related to the interplay between the amorphous entanglement density and the stability of crystal blocks. We report experimental evidence from true stress-strain experiments that support this argument. It is emphasized that tie molecules, which connect adjacent lamellae, are of lesser importance with respect to the deformational behavior.

DOI: 10.1103/PhysRevLett.91.095502

PACS numbers: 61.41.+e, 62.20.Fe, 81.05.Lg

Many polymers, such as, e.g., polyethylene, polypropylene, polyamide, etc. crystallize when being cooled from the melt. Differently from, e.g., metals, polymers crystallize only to a certain degree—typically between 10% and 50%—because the process is kinetically controlled [1]. In most cases crystalline lamellae are realized which are stacked periodically, with a periodicity of typically 10 to 50 nm. The lamellar crystals usually have a thickness of several to tens of nanometers and a lateral size of some micrometers. Since the polymer chains in the crystalline phase are oriented perpendicular to the lateral direction of the lamellae and their length is much larger than the lamellar thickness, there are numerous chains emanating from the crystalline lamellae into the interlamellar region thus forming an amorphous polymeric phase [2]. The polymeric chains in this interlamellar region are assumed to be highly entangled since most of the entanglements of the molten state are preserved upon rapid cooling [1,3]. Semicrystalline polymers exhibit large plasticity when being deformed above the glass transition temperature of the amorphous phase [4,5]. To account for this plastic nature, two general but distinctly different arguments have been proposed: first, it is suggested that the deformation is accomplished by slips within the lamellae including crystallographic fine slips and intralamellar mosaic block slips [6–8]; second, stress-induced melting and recrystallization was proposed to be responsible for the deformation process [3,9].

In recent years we have performed extensive investigations on the deformation mechanisms of semicrystalline polymers utilizing true stress-strain measurements at constant strain rate [10–15]. The true stress-strain curves together with detailed studies on the recovery properties yielded a surprisingly simple scheme for the process of tensile deformation in semicrystalline polymers: Along the true stress-strain curves, one always finds critical

points where the differential compliance and the recovery property change qualitatively. These critical points could be interpreted as (i) the onset of isolated inter- and intralamellar slip processes after the initial purely Hookean elastic range (point A), (ii) change into a collective activity of slip motions at the yield point (point B), and (iii) the beginning of destruction of crystal blocks followed by the formation of fibrils (point C). It was found that the strains at each point remain essentially constant for each class of polymer when varying crystallinity [10], temperature [11], and strain rate [11,13], as well as crystalline thickness [12].

In this Letter we consider the deformation mechanisms at point C. Three points will be clarified by comparing experiments on samples with varying entanglement density in the amorphous phase and different stabilities of the crystals: (1) The extension ratio at point C is directly related to the network modulus of the amorphous phase. (2) The deformation at point C is not related to the density of tie chains that connects adjacent crystals. (3) The critical stress for the destruction of the crystal blocks is related directly to the stability of the blocks.

Experiments.—To vary the entanglement density of the amorphous phase, we performed two sets of experiments. First, we chose poly- ϵ -caprolactone (PCL) and its miscible blends with second amorphous polymers poly(styrene-co-acrylitrane) (SAN) and poly(vinylmethylether) (PVME), respectively, where SAN and PVME mix with the amorphous phase of PCL only [16]. Second, we used polyamide 6 (PA6) and its copolymer PA6/66 (monomer ratio of 4:1 in mole) both in their dry and water saturated states. For the PA samples, the entangled amorphous state can be changed by water saturation or temperature variation because these changes affect the interchain hydrogen bonding interaction in the amorphous phase [17]. The critical strains at A and B, related

to the properties of the crystalline phase, remain constant for each system according to what was stated above [16,18]. In Fig. 1 the critical strain at C is derived from the results of free-shrinkage experiments for the

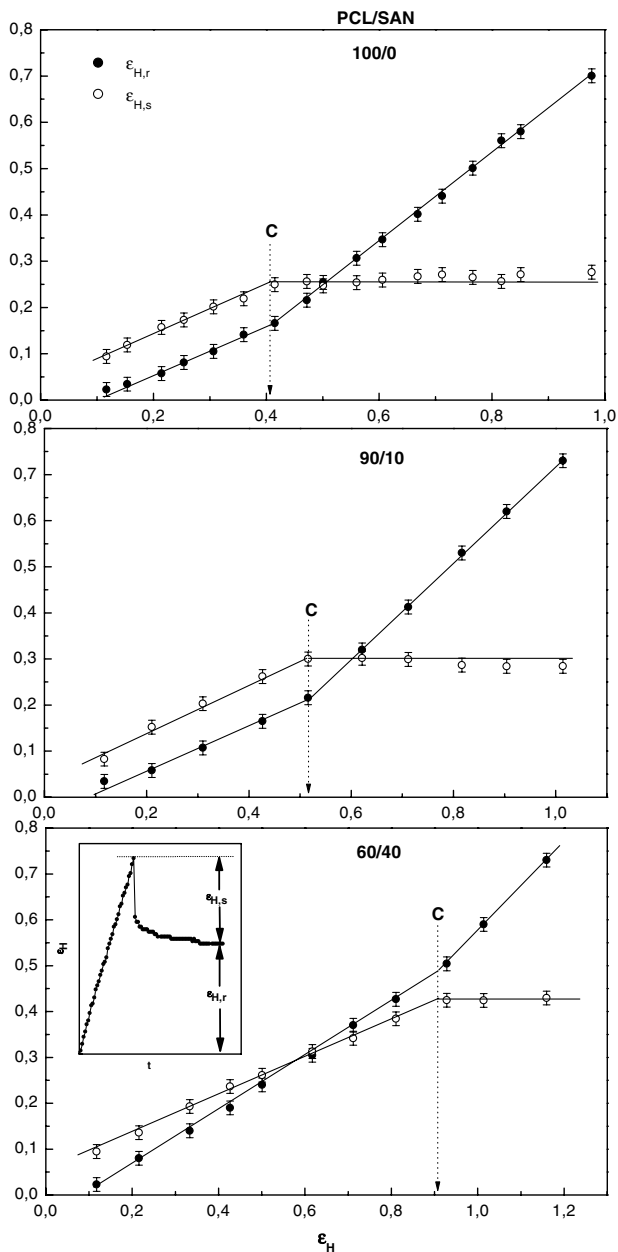


FIG. 1. Dependence of the shrinkage (elastic) part $\epsilon_{H,s}$, and plastic part $\epsilon_{H,r}$ of ϵ_H on the total strain, ϵ_H , for PCL/SAN blends. The dependence of the critical strain at point C on the content of SAN is clearly seen. Data are derived from free-shrinkage experiments. In such a measurement, the sample is first stretched to a certain strain ϵ_H and then the change in the strain is registered after a sudden release of the lower clamp. In such a way the total strain, ϵ_H , can be decomposed into a shrinkage (elastic) part $\epsilon_{H,s}$ and a plastic part $\epsilon_{H,r}$ as shown in the inset plot. The typical time scale in such an experiment is 10 min which ensures that the relaxation of the sample is nearly complete.

PCL/SAN blend (see the inset and the figure caption for experimental detail) as the point where the elastic strain reaches a plateau value. The dependence of the critical strain at C on the amount of SAN is clearly seen.

Modulus of the amorphous phase.—The network modulus can be extracted using the Gaussian model of Haward and Thakray [19,20] as shown in the inset of Fig. 2(b). In this model, semicrystalline polymeric material is represented as a Hookean elastic spring in a series with an Eyring dashpot and a rubbery spring [21] in parallel. This simple model describes all basic macroscopic effects that occur during stretching. The Hookean spring and the dashpot correspond to the crystalline phase including the block as well as the lamellar coupling and slips, respectively. The rubbery spring represents the entangled amorphous phase. Based on this model, a plot of the true stress as a function of $\lambda^2 - 1/\lambda$ should yield two lines with slopes yielding the Hookean elastic constant E and the rubber elastic constant G , respectively, where λ is the draw ratio. Figure 2 gives an example of such evaluation. Here, water saturated PA6 and PA6/66 were drawn at room temperature at

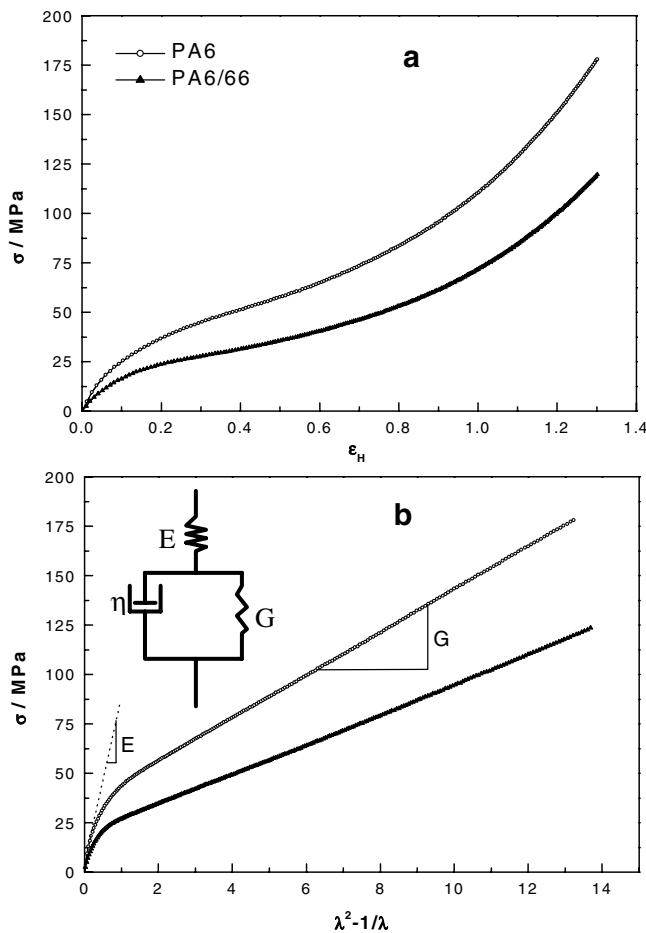


FIG. 2. True stress-strain curves of water saturated PA6 and PA6/66 at room temperature (a); the corresponding Haward-Thackray plots (b). The model is shown as an inset in the bottom figure.

a strain rate of $5 \times 10^{-3} \text{ s}^{-1}$ [18]. The true strain ϵ_H is related with λ by

$$\epsilon_H = \ln \lambda.$$

As can be seen, in Fig. 2(b), the determination of G is meaningful. Following the procedure exemplified in Fig. 2, we calculated the network moduli for the two sets of samples and collected the data in Fig. 3. Here, the reduced network modulus $G/(1 + 2.5\alpha_c)$ is used to remove the effect of crystallinity α_c by using the Einstein relation [22]. The crystallinity was determined by differential scanning calorimetry measurements according to standard procedures. The Einstein relation can be applied here because the crystallinity in the systems is low and the system can be treated as a filled rubber where the crystals are treated as the filling particles. This leads, for a given type of sample, to

$$\sigma_{nw}(C) = G/(1 + 2.5\alpha_c) \times (\lambda^2(C) - 1/\lambda(C)) = \text{const},$$

where $\sigma_{nw}(C)$ is the critical network stress at point C and $\lambda(C)$ is the extension ratio at point C. This relationship means that in a double logarithmic plot of $G/(1 + 2.5\alpha_c)$ as a function of $\lambda^2(C) - 1/\lambda(C)$ a straight line with a slope of -1 should be found for each type of sample. In the present case, this is indeed the case as indicated in Fig. 3. It should be noted that the PCL/SAN and PCL/PVME blends show different critical strain at C even if the SAN and PVME contents are the same. This is due to the difference in the molecular structure of SAN and PVME that affects the entanglement density of the

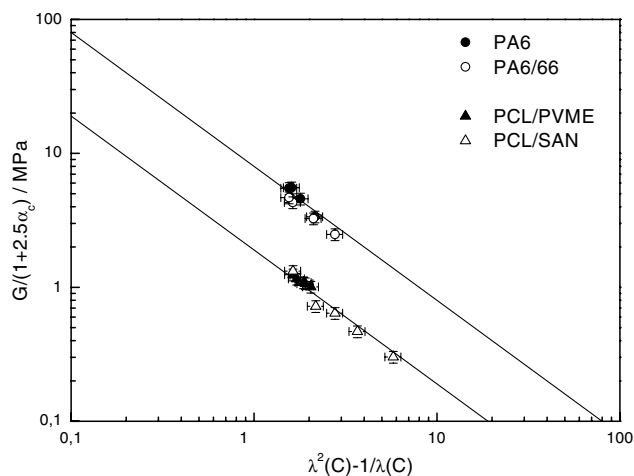


FIG. 3. Reduced network modulus $G/(1 + 2.5\alpha_c)$ as a function of $\lambda^2(C) - 1/\lambda(C)$ for PCL and PA6 systems. $\lambda(C)$ is the extension ratio at point C. The solid lines show the respective slope of -1 . In the case of PCL blends, the variation in entanglement density was achieved by blending different amounts of SAN or PVME (0, 10, 20, 30, and 40 wt %) with PCL. In the case of the PA samples, experiments were performed with water saturated samples at room temperature and with dry samples at elevated temperatures (80, 120, and 160 °C); the density of the interchain hydrogen bonds and thus the strength of the amorphous phase had been changed.

095502-3

system to a different extent. SAN with bulky phenyl side groups of styrene and a stiff main chain acts as an effective diluent of the entanglements in the blends, whereas PVME possesses a similar flexible chain structure as PCL and thus does not influence the entanglement density in the blends much.

Tie chains.—Another important issue to be learned from Fig. 3 is that it is the amorphous phase as a whole that determines the large deformation mechanism of the system, although one of the components is not linked to the crystals by polymeric chains. The connecting molecules between amorphous and the crystalline phases transfer the force generated by the orientation of the whole entangled amorphous phase to the crystal blocks but their number is less important. This result clearly excludes the long-standing assumption of the stretching of “tie molecules,” i.e., polymer chains that connect adjacent crystalline lamellae, being the sole factor determining the mechanical strength of the semicrystalline polymers when being drawn [23,24]. Following the “tie molecule stretching” scheme, one would expect a similar location of the critical strain at point C for the two blend systems, PCL/PVME and PCL/SAN, when the amount of the second amorphous components is the same because both systems possess similar crystalline and amorphous thicknesses and thus a similar tie molecule density [16]. In Fig. 3, it can be seen that this is not the case. For instance, the rubber extension ratio at point C [$\lambda^2(C) - 1/\lambda(C)$] for blends with 40% PVME and SAN varies from 2 to 6. It is thus clear that those amorphous chains that are not linked to the crystallites cannot recover to their isotropic state on the time scale of a drawing experiment. Thus they contribute also to the total stress, although the experiments are always conducted at a temperature higher than the glass transition temperature.

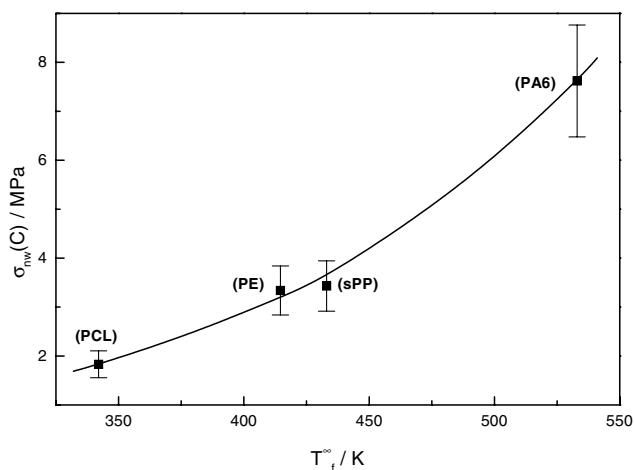


FIG. 4. Network stress at critical strain C as a function of the equilibrium melting temperature (from [26]) of systems studied. Data derived from Fig. 3 for PCL and PA6, from [10] for PE, and from [12,15] for sPP. The solid line serves as a guide for the eye.

095502-3

Experimental evidence for the orientation of this second type of amorphous chains in the crystalline miscible blends of PCL/SAN and PCL/poly (vinyl chloride) during deformation has been reported in literature [25].

Role of the crystalline phase.—The critical stress for destruction of crystal blocks must be related to the intrinsic stability of the crystal blocks. For a comparison between different systems we have studied, the equilibrium melting temperature (T_f^∞) (from [26]) was chosen as a measure of this stability. The values of $\sigma_{nw}(C)$ for different systems as a function of respective T_f^∞ is given in Fig. 4. Qualitatively, Fig. 4 supports our view because the critical network stress increases with increasing equilibrium melting temperature though one should be aware that T_f^∞ is determined by the melting enthalpy and the melting entropy, i.e., by the strength of the crystalline structure and the configurational degrees of freedom of the polymer in the amorphous state.

Deformation mechanisms.—Apparently, the two different arguments on the tensile deformation mechanism of semicrystalline polymer discussed in literature can be unified: Stretching of a semicrystalline polymer material can be viewed as a stretching of two interpenetrated networks being built up by interlocked lamellae (the crystalline phase) and the entangled amorphous phase, respectively [13,14]. Forces are first transmitted via the crystalline skeleton since the entangled melt is fluid (above its glass transition temperature). Block slips determine the critical strains at A and B. Further stretching leads to a gradual orientation of the amorphous chains along the drawing direction that decreases the entropy of the amorphous phase. A retracting force is always generated because the system tends to recover an isotropic state of optimized entropy [1,21]. This force is transferred to the crystallites via the molecules that link both phases. At point C, the stress acting on the crystallites reaches a critical value above which the crystalline blocks are no longer stable and the deformation mechanism changes from block slips into a disaggregation-recrystallization process [13,14]. The recrystallization process produces new crystallites in which the polymer chains are preferentially oriented along the drawing direction. An assembly of the oriented crystallites generally forms fibrils. Thus a sudden change in the recovery property is always observed at point C. It is easy to understand that the location of point C is governed by two factors, the modulus of the entangled melt and the stability of the crystal blocks.

In summary, we elucidated the role of the entangled amorphous phase in the tensile deformation process of semicrystalline polymers. Stretching of a semicrystalline polymer always results in a stretching of the interpenetrating networks of interlocked crystallites and the entangled amorphous phase. The amorphous network stretching begins to dominate the deformation process at a strain larger than the yield strain at which a critical

network stress is reached that starts to destruct the crystal blocks. It is shown that the interplay between the state of the amorphous phase together with the intrinsic stability of crystal blocks determines the position of the critical strain at this point. A higher entanglement density implies a higher stress that is generated when the sample is stretched. The more stable the crystallites the higher is the stress needed for their destruction. Because all the amorphous chains are oriented during stretching regardless whether they are linked with the crystallites or not, we exclude the possibility of mere tie molecule stretching but rather emphasize the role of the entangled amorphous phase as a whole in the process of deformation.

*Electronic address: yongfeng.men@basf-ag.de

- [1] G. Strobl, *The Physics of Polymers* (Springer, New York, 1997).
- [2] K. Kaji, *Applications of Neutron Scattering to Soft Condensed Matter* (Gordon and Breach Science Publisher, New York, 2000), p. 107, and references therein.
- [3] P. Flory and D. Yoon, *Nature (London)* **272**, 226 (1978).
- [4] I. Ward, *Mechanical Properties of Solid Polymers* (Wiley, New York, 1983).
- [5] L. Lin and A. Argon, *J. Mater. Sci.* **29**, 294 (1994), and references therein.
- [6] A. Peterlin, *J. Mater. Sci.* **6**, 490 (1971).
- [7] P. Bowden and R. Young, *J. Mater. Sci.* **9**, 2034 (1974).
- [8] R. Seguela and F. Rietsch, *J. Mater. Sci. Lett.* **9**, 46 (1990).
- [9] R. Popli and L. Mandelkern, *J. Polym. Sci. Polym. Phys. Ed.* **25**, 441 (1987).
- [10] R. Hiss, S. Hobeika, C. Lynn, and G. Strobl, *Macromolecules* **32**, 4390 (1999).
- [11] S. Hobeika, Y. Men, and G. Strobl, *Macromolecules* **33**, 1827 (2000).
- [12] Y. Men and G. Strobl, *J. Macromol. Sci. Phys. B* **40**, 775 (2001).
- [13] Y. Men, Ph.D. thesis, University of Freiburg, 2001.
- [14] Y. Men and G. Strobl, *Chin. J. Polym. Sci.* **20**, 161 (2002).
- [15] Y. Men, G. Strobl, and P. Wetter, *e-Polym. No.* **040** (2002).
- [16] Y. Men and G. Strobl, *Macromolecules* **36**, 1889 (2003).
- [17] J. Hirschinger, H. Miura, K. Gardner, and A. English, *Macromolecules* **23**, 2153 (1990).
- [18] Y. Men and J. Rieger (to be published).
- [19] R. Haward and G. Thackray, *Proc. R. Soc. London, Ser. A* **302**, 453 (1968).
- [20] R. Haward, *Macromolecules* **26**, 5860 (1993).
- [21] L. Treloar, *The Physics of Rubber Elasticity* (Clarendon Press, Oxford, 1975).
- [22] H. Smallwood, *J. Appl. Phys.* **15**, 758 (1944).
- [23] A. Lustiger and R. Markham, *Polymer* **24**, 1647 (1983).
- [24] M. Takayanagi and K. Nitta, *Macromol. Theo. Simul.* **6**, 181 (1997), and references therein.
- [25] D. Keroack, Y. Zhao, and R. Prud'homme, *Polymer* **40**, 243 (1998).
- [26] Athas database, <http://web.utk.edu/athas/databank/>